

Microstructural and electrical properties of (Sr,Ba)Nb₂O₆ thin films grown by pulsed laser deposition

Anna Infortuna, Paul Muralt*, Marco Cantoni, Alexander Tagantsev, Nava Setter

Ceramics Laboratory, Swiss Federal Institute of Technology EPFL, Lausanne 1015, Switzerland

Abstract

Strontium barium niobate thin films have been deposited by pulsed laser deposition on (111)-textured Pt films, p-doped Si(100) and Nb doped STO (SrTiO₃) single crystals. The deposition parameters were optimized for obtaining phase pure (001)-oriented films from stoichiometric targets. The samples were annealed in oxygen to improve top electrode adhesion and reduce oxygen vacancies. The SBN/substrate interfaces were investigated by means of TEM combined with EDAX chemical analysis. Growth on silicon resulted in the formation of a few nm thick SiO₂ interface layer. Epitaxial growth has been obtained on STO. A broad relaxor-type or diffuse phase transition occurs around -50 °C well below the transition temperature of single crystals. A second dielectric anomaly is observed around 80 °C, which, however, disappears after annealing in O₂. Above, the dielectric loss increases exponentially due to presumed leakage by ion conduction. Hysteresis loops at room temperature confirm relaxor-type behaviour with a saturation polarization of 18 $\mu\text{C}/\text{cm}^2$ and a weak hysteresis with a coercive field of 50 kV/cm.

© 2003 Elsevier Ltd. All rights reserved.

Keywords: Dielectric properties; PLD; SBN; Shifted phase transition

1. Introduction

Sr_xBa_{1-x}Nb₂O₆ (SBN_x) belongs to the family of ferroelectric materials with tetragonal tungsten bronze (TTB) structure (space group P4bm) and forms a solid solution in the range $0.25 < x < 0.75$. It exhibits very high electro-optic and pyroelectric coefficients as well as a good piezoelectric behaviour.^{1–3} The dielectric properties of single crystals depend strongly on the Sr/Ba content, ranging from normal ferroelectric at $x \leq 0.5$ to relaxor ferroelectric at $x > 0.5$.² The *para to ferroelectric* phase transition occurs in the range of 60–210 °C, increasing with increasing Ba concentration. Structure refinement studies relate the relaxor behaviour to the structural disorder, which was shown to be directly proportional to the Sr content.⁴ This tendency is related to the fact that the smaller Sr cation occupies the A1 (five-fold cavity) and A2 (four-fold cavity) sites in a random way, whereas the larger Ba ions are sitting on A1 sites only. Differences in measured values of dielectric constant and transition temperature can be attributed to different heat treatment histories of the material,

which is thought to affect the Sr site distribution. In polycrystalline SBN all the compositions behave like relaxor ferroelectrics and the transition temperature as well as the other properties are strongly dependent on sintering conditions.^{5,6} For thin films there are much less data available on electric properties. So far, SBN thin films have been grown by PLD,⁷ sputtering⁸ and sol-gel.⁹

2. Experimental

SBN50 and SBN60 thin films have been grown by pulsed laser deposition (PLD) from ceramic targets of the same composition. The targets have been prepared by mixing SrCO₃, BaCO₃ and Nb₂O₅ powders in acetone, calcinating at 1100 °C for 6 h, and sintering at 1350 °C for 12 h in air. The composition has been checked with X-ray fluorescence, confirming the correct value within an error of 1%. X-ray diffractograms reveal a mixture of SrNb₂O₆ and SBN phases.

Targets were ablated with a Lambda Physik ArF laser, 193 nm wavelength 10 Hz pulse repetition frequency and 2 J/cm² laser fluence. Several types of substrates have been used: amorphous SiO₂,

* Corresponding author. Fax: +41-2169-35810.

E-mail address: paul.muralt@epfl.ch (P. Muralt).

polycrystalline (111) Pt on SiO₂, p-doped Si(100) wafers (0.1–0.5 Ωcm) and conductive SrTiO₃ single crystals doped with 1%Nb. During deposition, the substrate temperature amounted to 740 °C and the oxygen pressure was varied between 10⁻¹ and 10⁻² mbar. The film thickness was typically 300 nm. When using conductive silicon as a substrate, the native oxide has been removed by etching in a 1% HF solution. The deposition was started at room temperature and the oxygen pressure was kept at a lower value, in order to reduce as much as possible the formation of a low dielectric constant interlayer by oxidation of silicon.

The film composition was correctly obtained, as measured with X-ray fluorescence (estimate error of 1%). For dielectric measurements, Pt top electrodes of 500 μm diameter were deposited by dc sputtering. The samples were placed in a Delta chamber 9023 allowing temperature scans in the range of -150 to 230 °C. Dielectric constant and loss have been measured by means of a HP 4284A LCR meter with an ac voltage of 20 mV amplitude in the frequency range of 100 Hz to 1 MHz.

For comparison of properties, ceramic samples have been prepared as well. Ceramics of pure TTB phase have been obtained by sintering in oxygen atmosphere at 1250 °C for time during 2 h. Despite of phase purity, the density achieved this way was not good enough for use as PLD targets. Higher densities have been achieved by sintering in air. The latter always led to the presence of a second phase of non-ferroelectric SrNb₂O₆, regardless of temperature and heating rate.

3. Results

3.1. Ceramics

The transition temperatures are in good agreement with the one of single crystals (80 °C SBN60, 120 °C SBN50 and 210 °C SBN30). Relaxor behaviour is found for all tested compositions (SBN60 SBN50 and SBN30). The dielectric constants (650 peak values at 1 kHz for all compositions) are lower than the values found in the literature of 2000–4000 (Refs. 6 and 10) and a dielectric anomaly associated with high loss is found at about 200 °C probably due to oxygen vacancies. For air sintered ceramics the phase transition is shifted down by 100 °C. The only apparent difference as compared with the oxygen sintered ceramics is the presence of the SrNb₂O₆ phase.

3.2. Structural characterization of thin films

SBN is an uniaxial ferroelectric with polarization along the [001] axis. Maximal dielectric properties are obtained along this direction. It is thus desirable to have

the polar axis [001] perpendicular to the film plane. A good (001) orientation has been obtained on SiO₂ at a substrate temperature of 700 °C with an oxygen pressure of at least 10⁻² mbar. In contrast, the deposition temperature has to exceed 735 °C on Si, Pt and STO substrates in order to achieve a good (001) orientation or texture. Fig. 1 shows that phase pure SBN (001) has been obtained on Pt (111) electrodes. Epitaxial growth has been obtained on STO. X-ray polar figures show three different orientations in the plane (see Fig. 2): the most intense peak correspond to the alignment of the SBN lattice with the STO one, the other two with a rotation of 36° and 54° away from STO lattice main axis. They correspond to two mirrored versions (45° ± 9°) of the same epitaxial relation. This relation between film and substrate can be explained assuming

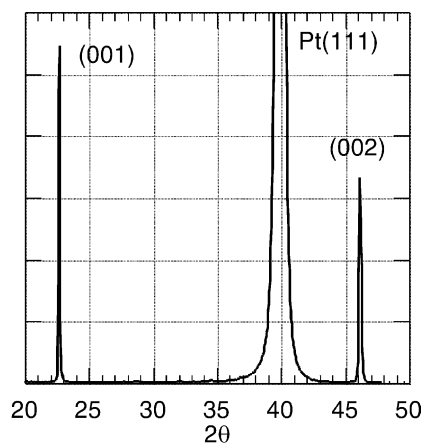


Fig. 1. θ - 2θ diffractograms for SBN50/Pt(111) film.

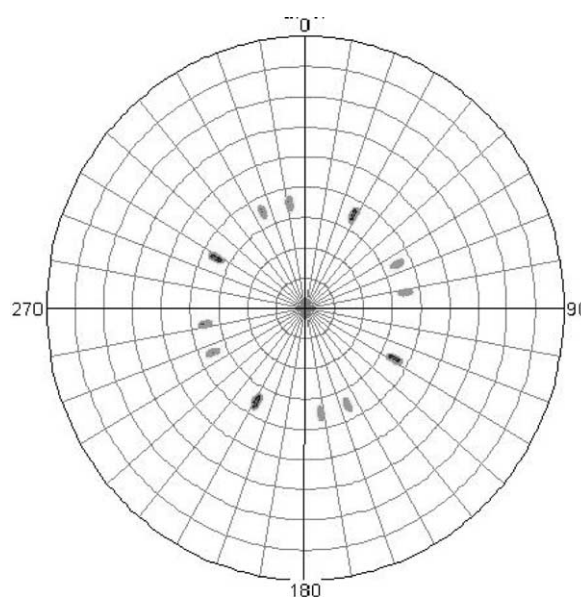


Fig. 2. Pole figure for SBN/STO of (211) reflections. (211) STO peaks are along the four bright spots.

that the four octahedra of the four-fold cavity—which form a perovskite geometry—are growing as continuation of the ST lattice.

SEM images show a relatively smooth surface. No particles are seen, as is often the case with PLD deposition. Film cross-section TEM images reveal columnar growth free of pores (Fig. 3). On Si substrates, an amorphous interface of a few nanometers (3–5) is clearly visible (Fig. 4). It consists of a mixture of Si and Nb oxide (EDAX analysis). The thickness of the amorphous interface layer exceeds the one (1 nm) of the initial layer deposited at room temperature, meaning

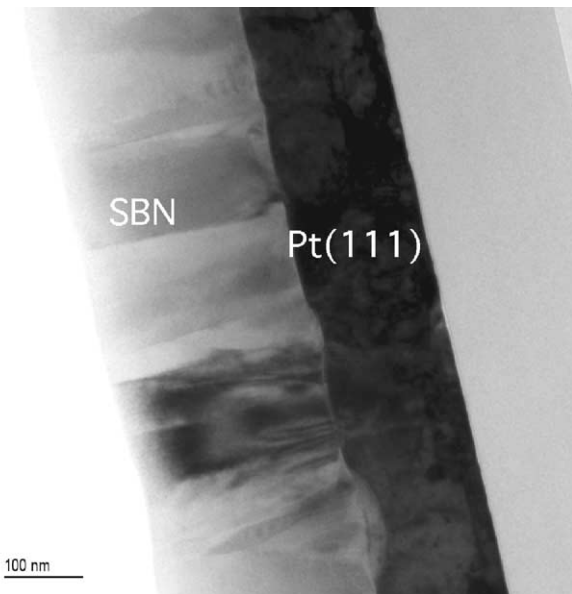


Fig. 3. TEM image of SBN60/Pt(111).

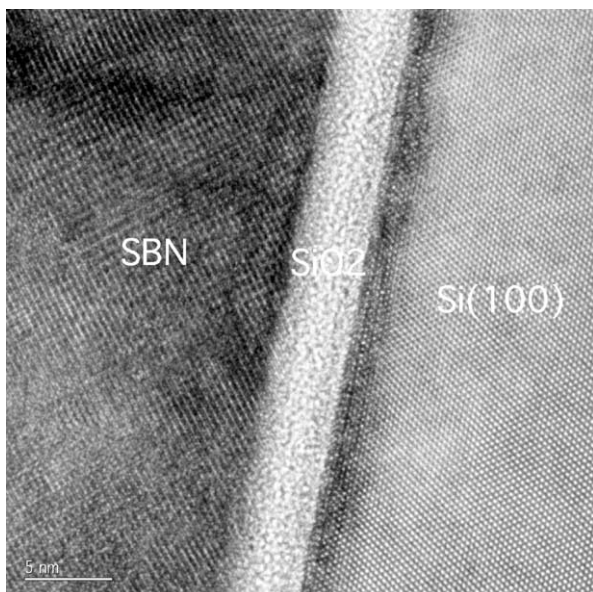


Fig. 4. High resolution TEM image of interface SBN60/Si(100).

that the interface is rather a result of inter-diffusion. Diffusion has been also observed in case of Pt substrates. Interface roughening and EDAX analysis reveals the existence of regions where the SBN is mixed with Pt and Ta from the adhesion layer.

3.3. Dielectric properties of thin films

Dielectric constant, as a function of temperature, has been measured on randomly and (001)-oriented films. Samples of SBN on Pt and STO (both composition SBN50 and SBN60) show two broad dielectric anomalies, one at temperature lower than -50 °C and the other at about 100 °C. The high temperature anomaly is broader, with a large dispersion in losses. This anomaly disappears after annealing in oxygen (rapid thermal annealing during 10 min). The required temperature amounts to 500 °C for SBN/STO and 700 °C for SBN/Pt. What is left after annealing is a broad phase transition of relaxor-ferroelectric type at about -50 °C for SBN on STO and -100 °C for SBN on Pt (see Fig. 5). The peak value of ϵ' amounts to typically 750. This

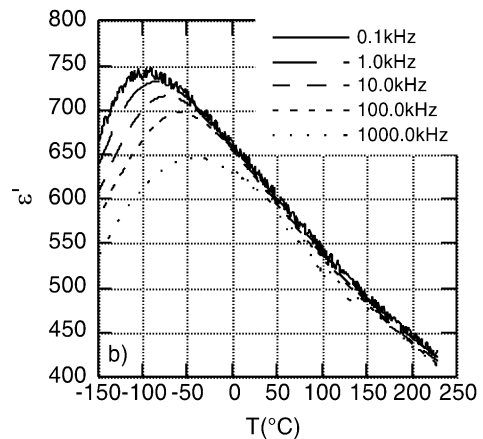
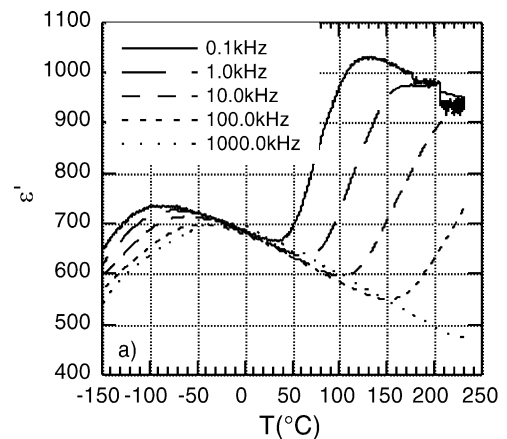


Fig. 5. Dielectric constant vs. temperature of SBN60/Pt(111) before anneal (top) and after anneal.

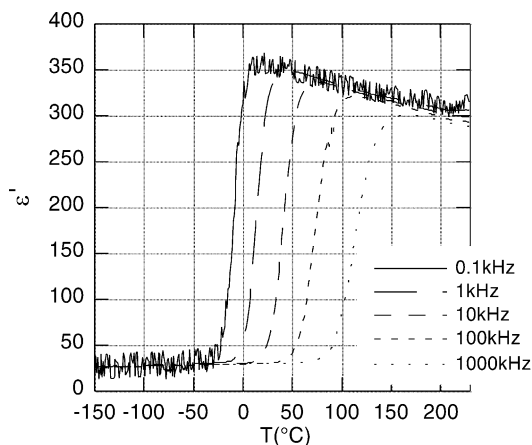


Fig. 6. Dielectric constant vs. temperature of SBN60/Si(100) after annealing.

value is comparable with the peak value measured at ceramics, although the latter occurs at much higher temperature.

Hysteresis loops (1 kHz triangular wave form applied field) measured at SBN/Pt samples show a ferroelectric hysteresis below and none above the phase transition. The dispersion in dielectric constant and loss indicate that this transition is of relaxor type. After annealing at 700 °C, room temperature behaviour is non linear (saturation of polarization) with no hysteresis. At –150 °C tilted ferroelectric loops with 17 kV/cm coercive field and 3 $\mu\text{C}/\text{cm}^2$ remanent and 14 $\mu\text{C}/\text{cm}^2$ saturation polarization are observed. The (001)-oriented samples on Pt show larger coercive field (40 kV/cm) at –150 °C. On STO, a coercive field is observed also at room temperature.

In the case of SBN on Si substrates, there are two superimposing dielectric anomalies around room temperature and around 100 °C, very broad and with a great dispersion. Annealing the sample in oxygen eliminates the one at 100 °C, the anomaly around room temperature remains (see Fig. 6). CV curves show the expected trends for p-doped silicon with high dielectric constants (200–300) at negative bias and small values (40–50) at positive bias. The lowering of the dielectric constant as compared to films on Pt electrodes can be explained by the 5 nm thick passive layer. A hysteresis effect is superimposed to the CV curve that is compatible with the idea that the ferroelectric SBN is poled at negative voltage when the p-doped silicon is the positive electrode, thus exhibiting minimal depletion width.

4. Discussion

Our study evidences two dielectric anomalies in electric measurement as function of temperature. The high

temperature anomaly is always found around 100 °C regardless of substrate used and texture of the materials. It is always possible to remove it with appropriate annealing in oxygen. It is broad with a large dispersion in both dielectric constant and loss, we conclude it is a Debye-like relaxation due to oxygen vacancies. Similar behaviour and results have been found in studies about perovskites.¹¹ There is evidence that the anomaly at low temperature corresponds to a relaxor-ferroelectric phase transition. The phase transition occurring in single crystals as well as in ceramics is very much suppressed in our films and shifted to much lower temperatures. We think that larger defect densities are the origin of such a behaviour.

It is known from single crystals that disorder on Sr and Ba sites leads to a lowering of the phase transition temperature (about 30° in SBN75).^{4,12} Long annealing steps are necessary to rearrange Sr and Ba atoms. There are as well reports on ceramics exhibiting phase transition that are 40–100° lower in temperature than in single crystals.^{6,10} We did not find any explanation for this phenomenon. All we may infer is that it can be due to defects related to grain boundaries. In thin films, there is in addition the interface to the substrate and a high density of grain boundaries (grain size about 100 nm wide and 300 nm long in our case). In our films such defects might originate from nucleation on a substrate that possesses a different structures than the film. The complexity of the tungsten–bronze easily allow dislocation during nucleation. In one unit cell of SBN there are essentially three differently oriented oxygen octahedra. This could cause a defective lateral ordering of the octahedra-chains especially at the low temperature used in PLD. To our knowledge only two article report the usual phase transition temperature for PLD deposited SBN films on Pt electrodes, and there are no apparent major differences with our processing parameters.^{7,13} However in these papers the frequency dependence of the supposed phase transition is not given, neither is the dielectric loss, and the dielectric constant has not been measured at low temperature. Further experiments are needed to clarify the reasons for the observed shift of the phase transition.

In the case of SBN on Si, dielectric measurements show the anomaly around RT (see Fig. 6), but no phase transition around –100 °C as in films on Pt. In this temperature range, the SBN dielectric behaviour is screened by low-dielectric phenomena related to the silicon interface with the passive layer. For explaining the observed behaviour one has to take into account the depletion layer in silicon, the passive oxide layer between silicon and SBN, and trapped charges at the interfaces of the amorphous layer. The anomalies shown in Fig. 6 are well compatible with charge relaxation of trapped charges and possibly related to the diffusion of charges through the passive layer.

References

1. Dorfer, U. B., A holographic method for the determination of all linear electrooptic coefficients applied to Ce-doped strontium-barium-niobate. *Appl. Phys B*, 1999, **68**(5), 843.
2. Glass, A. M., Investigation of the electrical properties of $\text{Sr}_{x-1}\text{Ba}_x\text{Nb}_2\text{O}_6$ with special reference to pyroelectric detection. *JAP*, 1969, **40**(12), 4699.
3. Neurgaonkar, R. R. et al., Piezoelectricity in tungsten bronze crystals. *Ferroelectrics*, 1994, **160**, 265–276.
4. Trubelja, M. P., Ryba, E. and Smith, D. K., A study of positional disorder in strontium barium niobate. *J. Mat. Sci.*, 1996, **31**, 1435–1443.
5. Desphande, S. B. et al., Preparation and ferroelectric properties of SBN:50 ceramics. *J. Am. Ceram. Soc.*, 1992, **75**(9), 2581.
6. Elissade, C. and Ravez, J., Relaxation mechanisms in $\text{Sr}_{0.3}\text{Ba}_{0.7}\text{Nb}_2\text{O}_6$. *J. Materials Chem.*, 2000, **10**, 681–683.
7. Kakimoto, K. et al., Synthesis and dielectric properties of $\text{Sr}_x\text{Ba}_{1-x}\text{Nb}_2\text{O}_6$ formed by YAG laser ablation. *J. Eur. Ceram. Soc.*, 2001, **21**, 1569–1572.
8. Yang, Y. S. et al., Ferroelectricity and electronic defect characteristics of c-oriented $\text{Sr}_{0.5}\text{Ba}_{0.5}\text{Nb}_2\text{O}_6$ thin films deposited on Si substrate. *Appl. Phys. Lett.*, 2000, **76**(23), 3472.
9. Xu, Y. et al., Ferroelectric $\text{Sr}_{0.6}\text{Ba}_{0.4}\text{Nb}_2\text{O}_6$ thin films by sol-gel process: electrical and optical properties. *Phys Rev B*, 1991, **44**(1), 35ss.
10. VanDamme, N. S. et al., Fabrication of optically transparent an electrooptic strontium barium niobate ceramics. *J. Am Cer Soc.*, 1991, **74**(8), 1785–1792.
11. Ang, C., Yu, Z. and Cross, L. E., Oxygen-vacancies-related low-frequency dielectric relaxation and electrical conduction in Bi:SrTiO₃. *Phys Rev B*, 2000, **62**(1), 228.
12. Chernaya, T. S., Atomic structure of $(\text{Sr}_{0.75}\text{Ba}_{0.25})\text{Nb}_2\text{O}_6$ single crystal and composition-structure-property relation in $(\text{SrBa})\text{Nb}_2\text{O}_6$ solid solutions. *Phys. of the Solid State*, 2000, **42**(9), 1668.
13. Cheng, H. F. et al., Ferroelectric properties of $(\text{Sr}_{0.5}\text{Ba}_{0.5})\text{Nb}_2\text{O}_6$ thin films synthesized by pulsed laser deposition. *Appl. Surf. Sci.*, 1997, **113/114**, 217–221.